Multimodality imaging of intrahepatic cholangiocarcinoma

Kelly Fábrega-Foster[1], Mounes Aliyari Ghasabeh[1], Timothy M. Pawlik[2], Ihab R. Kamel[1]

[1]The Russell H. Morgan Department of Radiology and Radiological Sciences Johns Hopkins University, 600 North Wolfe Street, MRI 143, Baltimore, Maryland, USA; [2]Department of Surgery, The Urban Meyer III and Shelley Meyer Chair in Cancer Research, The Ohio State University Wexner Medical Center, USA

Contributions: (I) Conception and design: None; (II) Administrative support: None; (III) Provision of study material or patients: None; (IV) Collection and assembly of data: None; (V) Data analysis and interpretation: None; (VI) Manuscript writing: All authors; (VII) Final approval of manuscript: All authors.

Correspondence to: Ihab R. Kamel, MD, Ph.D. The Russell H. Morgan Department of Radiology and Radiological Science, Johns Hopkins Hospital, 600 North Wolfe Street, MRI 143, Baltimore, MD 21287, USA. Email: ikamel@jhmi.edu.

Abstract: Intrahepatic cholangiocarcinomas account for approximately 20% of cases of cholangiocarcinomas. Three growth patterns or morphologic subtypes exist, including mass-forming, periductal-infiltrating, and intraductal-growth subtypes. Knowledge of these morphologic subtypes and their radiologic appearance aids in timely diagnosis, a key to optimizing patient outcomes. The morphologic variability of intrahepatic cholangiocarcinomas has a direct impact on the diagnostic sensitivity and specificity of various diagnostic imaging modalities, including ultrasound (US), computed tomography (CT), magnetic resonance imaging (MRI)/magnetic resonance cholangiopancreatography (MRCP), and positron emission tomography (PET). The following review emphasizes optimal imaging technique for each of these modalities and reviews the imaging appearance of each morphologic subtype of intrahepatic cholangiocarcinoma.

Keywords: Intrahepatic cholangiocarcinoma; mass-forming cholangiocarcinoma; periductal-infiltrating cholangiocarcinoma; intraductal cholangiocarcinoma

Submitted Jul 06, 2016. Accepted for publication Oct 09, 2016.
doi: 10.21037/hbsn.2016.12.10
View this article at: http://dx.doi.org/10.21037/hbsn.2016.12.10

Introduction

Cholangiocarcinoma is a primary biliary tract tumor arising from the bile duct epithelium (1). It is the most common biliary tract malignancy (2) and second most common primary hepatic tumor after hepatocellular carcinoma (2,3). While it accounts for less than 2% of all malignancies, it represents 10–15% of all primary liver cancers (4). Among gastrointestinal cancers, it is the most difficult to diagnose and therefore carries a poor prognosis with a 5-year survival rate of less than 10%. While most cholangiocarcinomas occurs sporadically, chronic biliary inflammation is a well known risk factor. Additional risk factors include primary sclerosing cholangitis (associated with ulcerative colitis in up to 86% of patients), choledochal cyst, familial polyposis, hepatolithiasis, congenital hepatic fibrosis, clonorchiasis, and a history of exposure to thorotrast (2,5). Diagnostic imaging, coupled with a high degree of clinical suspicion, play a critical role in timely diagnosis, staging, and evaluation for surgical resectability (6,7).

Classically, these tumors have been categorized according to their anatomic location as extrahepatic, peripheral intrahepatic, and hilar intrahepatic (1,2). Peripheral intrahepatic cholangiocarcinomas arise beyond the second-order bile ducts, accounting for 20% of cases. Perihilar intrahepatic cholangiocarcinomas arise from the confluence of the right and left hepatic bile ducts, accounting for 50–60% of cases. Distal extrahepatic cholangiocarcinomas arise from the bile duct below the level of the cystic duct insertion down to the ampulla of Vater (8). The anatomic location of the tumor is an important consideration for treatment planning and often reflects the clinical symptomatology (2).

According to a classification scheme proposed by the Liver Cancer Study Group of Japan, cholangiocarcinomas may also be classified according to their growth pattern or morphologic subtype as mass forming, periductal-infiltrating, or intraductal (9). Morphology is a useful indicator of the tumor's behavior and clinical outcome, often dictating the surgical approach (1,2,8). The mass-forming subtype invades the hepatic parenchyma, spreading along portal venous channels (1). The periductal-infiltrating subtype grows longitudinally along the bile duct walls, spreading via lymphatic vessels. The intraductal subtype proliferates focally within the biliary duct lumen, leaving the wall intact (1,2,4,8). While all three subtypes may occur at an intrahepatic location, certain morphologies predominate at certain sites. For instance, the mass forming subtype is the most common type of intrahepatic cholangiocarcinoma (10). Importantly, this anatomic and morphological variability impacts the diagnostic sensitivity and specificity of imaging modalities.

The most common imaging modalities used to diagnose and stage intrahepatic cholangiocarcinoma include ultrasound (US), computed tomography (CT), magnetic resonance imaging/magnetic resonance cholangiopancreatography (MRI/MRCP), and positron emission tomography (PET). The following chapter will review the role of each of these imaging modalities in the diagnosis and staging of intrahepatic cholangiocarcinoma. We will emphasize optimal imaging technique for each modality and review the imaging appearance of each morphologic subtype of intrahepatic cholangiocarcinoma.

Imaging technique

Ultrasound (US)

Ultrasound is often the first imaging modality employed in patients with obstructive jaundice or abdominal pain. In addition to detection of cholangiocarcinoma, it helps to exclude more common etiologies for obstructive jaundice such as choledocholelithiasis. A curved linear array transducer in the 2–6 MHz range is usually needed to evaluate the liver parenchyma. A higher frequency transducer in the 7–12 MHz range is used to evaluate the liver surface for nodularity, an ancillary imaging feature of cirrhosis.

The diagnostic accuracy of ultrasound is improved by the use of ultrasound contrast agents. Three ultrasound contrast agents are currently employed worldwide and have been recently FDA approved. Two of these are vascular agents and do not diffuse outside of vessels, providing only information about the early dynamic enhancement pattern of biliary lesions. A third agent is taken up by Kupffer cells in the liver and exhibits a hepatobiliary phase 1 hour after injection, with a utility similar to that of the hepatobiliary agents utilized in MRI (11). This may be useful for distinguishing intrahepatic forms of cholangiocarcinoma from hepatocellular carcinoma (12).

Histopathologically, imaging findings of cholangiocarcinoma on CE-US correlate with the degree of carcinoma cell proliferation. Hyperenhancing areas on CE-US indicate increased density of cancer cells, whereas hypoenhancing areas indicate the presence of fibrous stroma. Different distributions of cancer cells within alesion therefore correspond to different contrast-enhancement patterns. The distribution of cancer cells within a given lesion also provides clues about its blood supply, since cancer cells are most likely to proliferate in areas with abundant blood supply. Hence the enhancement pattern on CE-US may be helpful both in diagnosis and treatment planning of intrahepatic cholangiocarcinoma (13).

Intraoperative ultrasound serves as a valuable tool to guide surgical technique during resection of cholangiocarcinoma (14,15). The Couinaud classification of anatomical and functional liver anatomy divides the liver into segments based on portal and hepatic venous anatomy; these segments are readily identifiable by ultrasound and assist in targeted segmental resection. Intraoperative ultrasound can also be used to detect intrahepatic biliary stones to ensure their removal (16), as well as to guide other forms of oncological treatment, such as radiofrequency ablation (17).

Computed tomography (CT)

Multiphase contrast-enhanced computed tomography (CE-CT) is widely utilized to diagnose and stage cholangiocarcinoma. Not only does it assist in characterization of liver masses and detection of biliary ductal dilatation, but it also demonstrates associated prognostic features such as vascular encasement and nodal involvement. Non-contrast CT may be used as a part of a more comprehensive contrast-enhanced imaging protocol and may be helpful in differentiating radiodense intraductal biliary stones from an enhancing intraductal mass (18,19).

A typical contrast-enhanced protocol for diagnosis and initial staging of cholangiocarcinoma includes arterial (20–30 sec post-injection) portal venous (60 seconds

post-injection), and delayed (at least 3 minutes post-injection) phases (20,21). The arterial phase not only helps to distinguish hepatocellular carcinoma from cholangiocarcinoma (the former is more likely to demonstrate arterial enhancement), but also helps more clearly to delineate the vascular anatomy prior to surgical resection. The delayed phase, performed at 3–10 minutes after contrast injection, accentuates the presence of fibrous stroma, which is a distinguishing feature of cholangiocarcinomas (20,21).

Most primary hepatocyte tumors receive preferential blood supply from the hepatic arteries, while healthy liver parenchyma receives the majority of its blood supply from the portal vein. This difference is reflected in the enhancement pattern of intrahepatic tumors and aids in distinguishing primary hepatocyte tumors from background parenchyma, as well as differentiating subtypes of intrahepatic tumors. A classic example of this is the differential enhancement pattern of hepatocellular carcinoma (HCC) *vs.* intrahepatic cholangiocarcinoma. Unlike primary hepatocyte tumors, intrahepatic biliary tumors often remain centrally hypoattenuating (with or without rim enhancement) relative to the liver parenchyma in the arterial and portal venous phases, enhancing most prominently in the delayed phase, a feature which reflects their desmoplastic nature (2). The degree of desmoplasia in an intrahepatic cholangiocarcinoma is not only distinctive, but also has prognostic implications (22-24). Specifically, intrahepatic cholangiocarcinomas that are hypovascular in the hepatic arterial phase are more likely to demonstrate lymphatic, perineural, and biliary invasion such that tumor hypervascularity may serve as an independent pre-operative prognostic factor for disease free survival (25).

MRI/MRCP

Compared with MRI, CE-CT has a limited ability to detect spread of tumor along bile ducts (8). MRI excels at this task due to its superior soft tissue contrast and is therefore considered the imaging modality of choice for diagnosis and staging of cholangiocarcinoma. Its accuracy is similar to that of CE-CT and direct cholangiography combined (8).

An optimal protocol for cholangiocarcinoma evaluation should include MRCP, conventional T1- and T2- weighted abdominal MRI pulse sequences (including T1 in- and out-of-phase imaging), diffusion weighted imaging (DWI), and multiphase contrast-enhanced sequences obtained in the arterial, portal venous, and delayed phases (6,8). These post-contrast sequences may be obtained at pre-determined time points or with bolus tracking technique (6).

Magnetic resonance cholangiopancreatography (MRCP) is the most accurate, non-invasive method for assessment of the biliary system (8). MRCP is a non-contrast MR technique in which the T2-weighted contrast between bile (long T2) and adjacent tissues (short T2) is accentuated by using heavily T2-weighted sequences. Thin multi-slice MRCP allows high-resolution visualization via three dimensional image data sets (8). Unlike endoscopic retrograde cholangiopancreatography, MRCP is non-invasive and allows visualization of the biliary ducts proximal to an obstruction (26). In preparation for MRCP, patients fast for at least 4 hours to minimize bowel peristalsis and gastric secretions and maximize gallbladder distention. Negative contrast agents can also be added to reduce fluid signal in the stomach and duodenum (26). DWI may assist MRCP in detecting tumor within dilated or obstructed ducts when contrast injection is not possible (8).

It is well documented that DWI increases the diagnostic sensitivity of MRI for cholangiocarcinoma. Previous studies have documented overlap in the dynamic contrast enhancement patterns of small mass-forming intrahepatic cholangiocarcinomas (<3 cm) and hepatocellular carcinomas (18,27). In such cases, diffusion weighted imaging performed at a number of different b-values ranging from 0–800 s/mm^2 may help to distinguish ICC from HCC (28,29). Similarly, DW-MRI may assist in distinguishing benign from malignant strictures, which is critical for diagnosis of periductal infiltrating subtypes of ICC (30).

Generally speaking, the ADC values of ICCs tend to be significantly lower than that of the adjacent normal hepatic parenchyma, as is the case for most malignant hepatic tumors. Documentation of a range of ADC values specific for ICC has been limited by wide variability in reported ADC values. This variability, largely attributable to differences in image acquisition technique, has prompted researchers to advocate for the use of normalized ADC values for optimal quantitative characterization of liver lesions, including ICC. Qualitatively, however, studies have shown that DW-MRI yields the best conspicuity of ICC compared with other MRI sequences across a wide range of b-values. In one study, all cholangiocarcinomas were visible at b=0 s/mm^2 and the majority remained hyperintense on DW-MRI acquired at increasing b-values, suggesting that the use of the former b value should be considered in MR protocols for cholangiocarcinoma detection. This same study suggested that normalization to the background liver

parenchyma resulted in minimal variability in ADC values compared with other index organs such as the spleen (28).

The degree of diffusion restriction on DW-MRI may serve as an independent pre-operative prognostic marker in patients with intrahepatic cholangiocarcinoma. In one study, patients in whom less than one-third of the tumor showed diffusion restriction demonstrated more advanced initial TNM staging, more frequent lymphatic invasion and lymph node metastases, and more abundant stromal metaplasia compared with patients in whom more than one- third of the tumor showed diffusion restriction. Both disease-free and overall survival were significantly lower in the first group of patients compared with the second (31).

PET imaging

18F-Fluoro-2-deoxy-D-glucose (FDG) integrated positron emission tomography (PET) is a non-invasive imaging technique that allows *in vivo* assessment of the metabolic processes underlying malignant disease (32). Cancer cells are hypermetabolic, a fact which PET imaging exploits for imaging purposes. In PET imaging, patients are injected with a radiolabelled tracer that physiologically mimics glucose in the body, namely FDG. Membrane glucose transporter proteins (GLUT1) transfer glucose into the tumor cells. FDG is then phosphorylated by hexokinase 2 to FDG-6-phosphate, which has limited extracellular diffusivity. Because cancer cells overexpress the membrane transport proteins responsible for intracellular glucose uptake and sequestration (namely GLUT-1 and hexokinase), this results in relative increases in glucose metabolism compared with normal cells- a functional characteristic that is reflected in the form of imaging "hot spots" on the PET scan (3,33). Importantly, all types of cholangiocarcinoma will be FDG avid on PET.

Although PET alone has limited spatial and temporal resolution, these limitations are compensated for by coupling with low dose multidetector CT. The sensitivity and specificity of PET-CT for diagnosis of cholangiocarcinoma varies by location and is higher for intrahepatic (>90%) than extrahepatic (about 60%) cholangiocarcinomas (34). The detection rate of distant metastases approaches 100%.

Both CT and MRI demonstrate limited sensitivity and specificity for positive nodal metastases (11). MRI with MRCP has a reported accuracy of 66% or lymph node metastasis. Some studies suggest PET-CT may improve nodal staging and identification of distant metastases, altering clinical management in up to 17–30% of patients (11). For this reason, PET-CT is recommended for pre-operative staging of both intra- and extra-hepatic cholangiocarcinomas. There is also some evidence supporting a prognostic role for PET-CT. Recent studies have shown that the preoperative SUV max serves as an independent risk factor for recurrence of cholangiocarcinomas (35).

Morphological subtypes

Mass-forming subtype (mCCA) (Figures 1,2)

Among intrahepatic cholangiocarcinomas, the mass-forming subtype (mCCA) is the most common, accounting for 80% of intrahepatic cholangiocarcinomas (2). The remaining 20% consists of periductal-infiltrating and intraductal-growth subtypes combined. mCCAs arise via spread through venous and lymphatic channels (2).

US

On ultrasound, mCCA appears as a homogeneous mass with intermediate to increased echogenicity and a peripheral hypoechoic halo (18). Usually tumors greater than 3 cm in size are hyperechoic, while smaller tumors are iso- to hypoechoic (36). A hypoechoic halo, visible in about 15% of tumors, represents a rim of proliferating tumor cells with compressed adjacent liver parenchyma (36). The shape of the mass may be irregular but the margins are typically circumscribed and associated capsular retraction may be sonographically visible (37).

On CE-US, mCCA may demonstrate early enhancement with subsequent washout mimicking HCC. Therefore, CE-US is not recommended as the sole imaging technique for conclusive diagnosis of mCCA (2).

CT

On unenhanced CT, mCCA presents as a homogeneously hypo- to isoattenuating mass with lobulated margins (2,38,39). After administration of iodinated contrast, the pattern of enhancement may be somewhat variable but is usually an accurate reflection of the histologic composition of the mass. Generally speaking, the periphery of the tumor is composed of active tumor cells, whereas the center of the tumor is composed of desmoplastic stroma, necrotic tissue, or mucin (2,18,38,39).

The majority of lesions demonstrate incomplete peripheral enhancement in the arterial phase that may

Figure 1 Mass-forming intrahepatic cholangiocarcinoma in a 59-year-old male. Ultrasound in the coronal plane (A) shows a hypoechoic mass (arrow) in the left lobe of the liver without evidence of intrahepatic ductal dilatation; (B) transverse unenhanced CT of the liver shows a subtle mass in segment IVB (arrow); (C) the mass (arrow) remains subtle in the portal venous phase of iodinated contrast enhancement, with intense metabolic activity on F-18 FDG PET (D); (E) transverse fat saturated T1-weighted MR image without iodinated contrast shows a slightly hypointense mass (arrow). T2-weighted image (F) shows a slightly hyperintense mass (arrow). On fat saturated post-gadolinium chelate T1-weighted image (G) the mass is hypervascular with rim enhancement (arrow). The mass (arrow) becomes isointense to liver parenchyma in the portal venous phase (H), and slightly hyperintense to liver parenchyma on the 5-minute delayed phase (I). Delayed enhancement is likely due to the presence of fibrous stroma, a distinguishing feature of cholangiocarcinoma. No intrahepatic ductal dilation is identified.

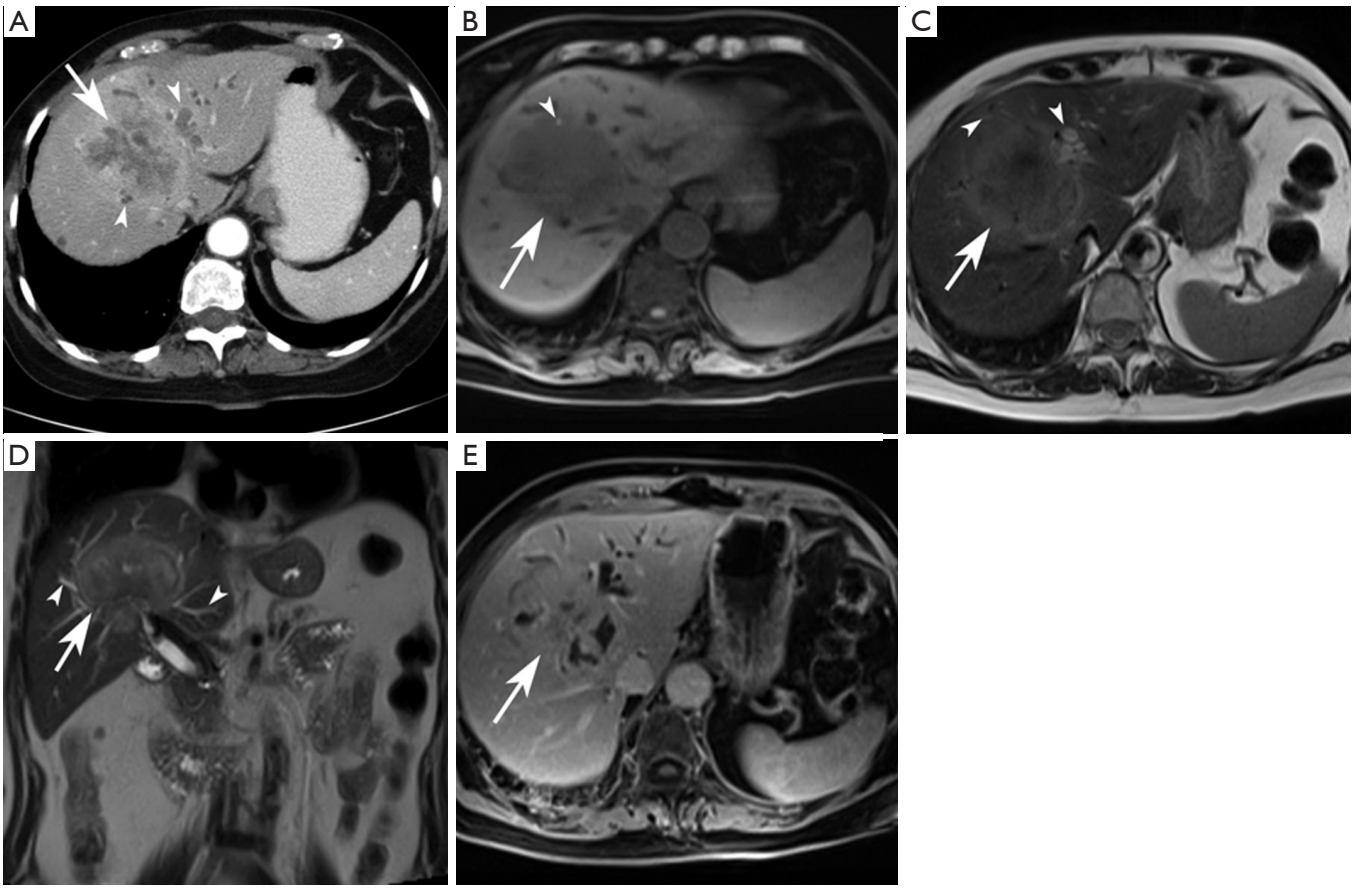

Figure 2 Mass-forming intrahepatic cholangiocarcinoma in a 73-year-old female. (A) Transverse post-iodinated contrast CT images obtained in the portal venous phase reveal a large, central liver mass (arrow) resulting in moderate intrahepatic ductal dilatation (arrowheads). The mass demonstrates rim enhancement and central necrosis; (B) transverse fat saturated T1-weighted MR image without iodinated contrast shows a hypointense mass (arrow). Notice the hyperintense signal (arrowhead) due to debris retained within moderately dilated intrahepatic ducts; transverse (C) and coronal (D) T2-weighted images show a slightly hyperintense mass (arrow) causing ductal dilation (arrowheads) in both lobes, particularly on the left; (E) transverse fat saturated post-gadolinium chelate T1-weighted image in the portal venous phase shows a large infiltrative hypovascular mass (arrow) with central necrosis.

become iso- or hypodense in the portal venous phase (32). The central fibrous stroma enhances most prominently in the delayed phase (39), unless there is abundant central mucin or necrosis. With necrotic or mucin-producing tumors, the central portion does not enhance in the late phase and remains hypodense throughout all three phases (2). The pattern of enhancement does depend, to some degree, on tumor size. Very small tumors (less than 1 cm in size) may demonstrate homogenous arterial phase enhancement, mimicking HCC (2). However, the presence of washout on the venous and delayed phases may help to distinguish HCC from subcentimeter mCCAs.

The degree of enhancement on delayed phase images not only helps to distinguish mCCA from HCC, but also has prognostic value. One study demonstrated that tumors which demonstrated delayed enhancement over greater than two-thirds of their volume had increased fibrous stroma and a higher incidence of perineural invasion, which is a poor prognostic maker (32,38,40,41).

Ancillary features of mCCA on cross-sectional imaging include capsular retraction, biliary obstruction and hepatolithiasis, satellite nodules, vascular encasement, lobar atrophy, and lymphadenopathy (32). Capsular retraction is an imaging feature originally described on CT that is not only associated with cholangiocarcinomas but a variety of other malignant hepatic tumors. In the setting

of cholangiocarcinoma, it may be difficult to distinguish from lobar or segmental atrophy secondary to vascular involvement (42). Dilated biliary ducts with intraductal stones may be found distal to the mass (40). In one study, the incidence of vascular encasement or compression was 82% for peripheral cholangiocarcinomas (43). Narrowing of the portal and/or hepatic veins may be present, but there is rarely vascular invasion with tumor thrombus formation (Han JK). While portal vein invasion has been described in the literature as a rare cause of portal venous hypertension (44), the presence of vascular invasion and tumor thrombus formation most commonly serves as a useful differentiating feature from HCC when the pattern of enhancement is equivocal (43). Vascular encasement or narrowing frequently results in atrophy of the involved hepatic segment (45) with or without associated capsular retraction (39), found in approximately 21% of patients (32).

Lymphadenopathy may be seen in up to 73% of cases, predominately affecting the portacaval and porta hepatis lymph nodes (43).

MRI

On T1-weighted images, mCCA presents as a hypo- to isointense mass. It may be mild to moderately hyperintense on T2-weighted images, depending on the relative proportions of central fibrous stroma *vs.* extracellular mucin (8,32). The dynamic enhancement pattern after gadolinium-based contrast administration is similar to CT and may be variable. As with CT, the most common pattern is a thin peripheral rim of enhancement in early arterial phase with progressive centripetal enhancement on the delayed phase. In predominantly fibrotic tumors, enhancement may only be visible in the delayed phase. Very small tumors may display intense homogeneous arterial enhancement with persistent enhancement into the delayed phase (8), but this pattern is less common and has been described on MRI in approximately 30% of peripheral mCCAs (43).

Ancillary features of mCCA described on CT have also been described on MRI, including vascular encasement, biliary obstruction, lobar atrophy, capsular retraction, and lymphadenopathy (8). However, the more peripheral the mCCA, the less likely it is to present with biliary obstruction, because tumors arise from and infiltrate along distal intrahepatic bile ducts (43). T1- and T2-weighted fat suppressed images are particularly helpful for detection of lymphadenopathy.

Post-contrast imaging may be performed with traditional gadolinium-based, extracellular contrast agents (Gd-DTPA) or derivatives such as gadolinium ethoxybenzyl diethylenetriamine pentaacetic acid (Gd-EOB-DTPA). Gd-EOB-DTPA combines features of a conventional extracellular gadolinium-based contrast agent and hepatocyte-specific contrast agents. Previous studies have documented the superiority of Gd-EOB-DTPA in detecting and characterizing hepatic lesions in patients with a background of diffuse liver disease. Because the post-contrast signal intensity of the liver is greater with the use of hepatocyte-specific agents such as Gd-EOB-DTPA compared with traditional gadolinium-based extracellular contrast agents, cholangiocarcinomas become increasingly conspicuous, appearing as hypointense on both early and delayed phase sequences (46). This provides a sharp contrast between the lesion and the liver background, allowing more accurate assessment of tumor extent, as well as the presence of associated satellite lesions which are seen in 10–20% of cases of mCCA (46). The increased conspicuity of cholangiocarcinomas in this setting is particularly helpful for patients with a background of diffuse liver disease, in whom mCCAs may exhibit atypical enhancement patterns after administration of traditional gadolinium-based extracellular contrast agents (47).

The use of Gd-EOB-DTPA may also unmask distinctive enhancement patterns in CCA. In one study, 93% of mCCAs displayed an "EOB cloud": a cloud-like central signal intensity with a perilesional hypointense rim on the hepatobiliary phase. The hypointense perilesional rim appears as an enhancement defect compared with the avidly enhancing background liver, and is thought to be attributable to regional cholestasis (47).

With Gd-EOB-DTPA, the relative signal intensity of the liver and visibility of the biliary tracts on the hepatobiliary phase may also serve as quantifiable, surrogate markers of biliary function. Gd-EOB-DTPA is taken up by hepatocytes and excreted into the biliary system. Decreased signal intensity of the background liver and reduced visibility of the biliary tracts on the hepatobiliary phase indicate impaired biliary function and may be quantitatively correlated with total bilirubin levels (46).

While first described as a characteristic pattern of contrast enhancement seen with intrahepatic mass-forming cholangiocarcinomas, the "target sign" is also a feature of mass-forming ICC that is visible on DWI. The "target sign" describes a pattern of progressive and concentric central enhancement with peripheral washout on delayed MRI performed at 1–4 hours with Gadopentetate dimeglumine or Gadobenate dimeglumine (29). On DWI, a

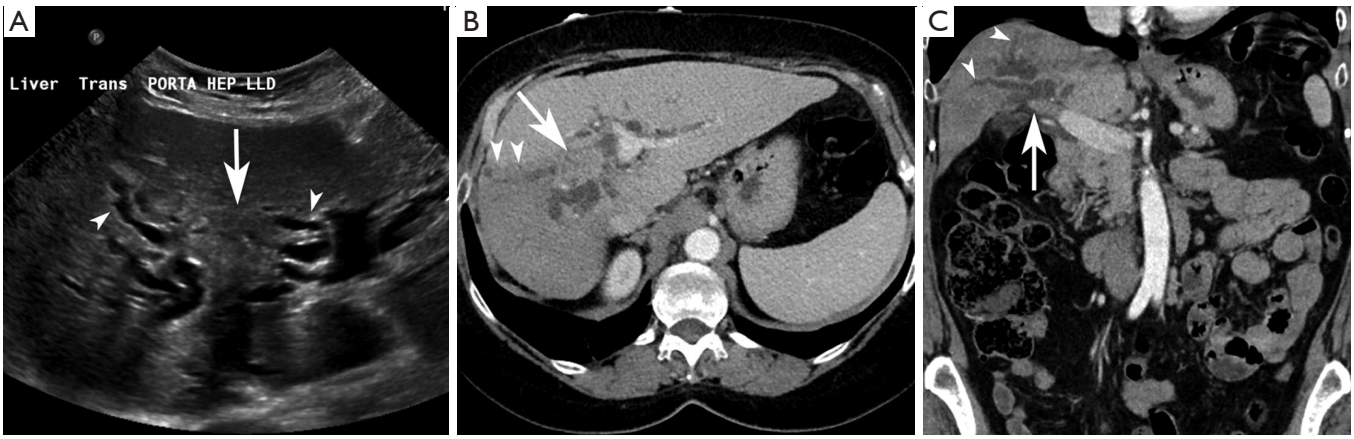

Figure 3 Periductal-infiltrating cholangiocarcinoma in a 65-year-old female. (A) Ultrasound of the right upper quadrant shows subtle perihilar infiltration (arrow) and intrahepatic ductal dilatation (arrowheads); (B) transverse post-iodinated contrast CT in the portal venous phase shows perihilar infiltration (arrow) and perfusion changes (arrowheads) resulting from an occluded right portal vein; (C) coronal CT shows an occluded right portal vein (arrow) and moderate intrahepatic ductal dilatation (arrowheads).

central hypointense area with a targetoid appearance is also seen at a number of b-values ranging from 0 to 800 s/mm^2. In one study, the presence of a target sign on high b-value DWI (b=800 s/mm^2) proved to be the most discriminating feature between mass-forming ICC and HCC (29).

Periductal-infiltrating subtype (piCCA) (Figure 3)

The majority of periductal-infiltrating cholangiocarcinomas (piCCA) are perihilar intrahepatic in location (2) but may arise at any point between the second order biliary ducts and the insertion of the cystic duct (2). PiCCA is also known as "sclerosing" because it grows along the bile duct walls resulting in alterations of biliary ductal caliber. An eponymous type of piCCA, known as a Klatskin tumor, arises at the bifurcation of the common hepatic duct into the right and left hepatic ducts (2,48).

US

The primary role of ultrasound in this setting is to rule out benign causes of biliary obstruction. Ultrasound rarely allows direct visualization of piCCA, unless it is associated with mass formation. However, indirect signs such as alterations in biliary caliber may be sonographically visible (2,49). The sensitivity and specificity of ultrasound for diagnosing perihilar forms of cholangiocarcinoma are 89% and 80–95%, respectively (2).

PiCCAs are characterized by biliary ductal thickening and/or altered biliary duct caliber in the absence of a discrete mass (23,48). Bile duct lumens may be obliterated depending on the degree of ductal involvement (50,51).

CT

Multidetector CT (MD-CT) and high resolution CT (HR-CT) play an increasingly important role in the diagnosis and staging of piCCAs. Fast scanning times, thin collimation, and excellent spatial resolution allow improved visualization of the longitudinal and radial extension of the tumor (49).

On CT, piCCAs present as thickening of the periductal parenchyma with narrowing or dilatation of bile ducts. Because the majority of these are present near the hilum, they usually cause segmental dilatation of the biliary tree (45,52). Segmental or lobar biliary ductal dilatation is an important differentiating feature from periportal lymphangitic metastases arising from an extrahepatic source. In contrast to periductal-infiltrating cholangiocarcinomas, lymphangitic metastases will not cause lobar or segmental ductal dilatation (23,45).

CT may show focal mural thickening, luminal obliteration, and proximal biliary ductal dilatation. Periductal thickening may be associated with a mass, liver atrophy, vascular encasement, lymphadenopathy, and distant metastases (53). About 80% of piCCAs demonstrate arterial and portal venous enhancement and most demonstrate prominent delayed phase enhancement due to their sclerosing histology (53).

CT cholangiography, wherein contrast is introduced

into a pre-existing biliary drainage site, is superior to conventional CT or US and equal to ERCP in diagnosis of piCCA, and is considered in patients in whom MRCP is contraindicated or unavailable (2).

MRI

MRI with MRCP is the considered the best non-invasive imaging option for diagnosis of extrahepatic and intrahepatic perihilar cholangiocarcinomas (11). It permits visualization of malignant stricturing with or without an associated mass, provides staging information such as the degree of vascular or ductal involvement, and allows accurate lesion characterization (11). The reported accuracy of MRCP for determining the longitudinal extent of bile duct involvement ranges between 71–96% (2,11). With MRCP, there is also better assessment of the extent of peripheral ductal involvement than with ERCP, wherein visualization of peripheral bile ducts may be limited by more central biliary obstruction (2). Acquisition of 3D MRCP image sets further assists in pre-surgical planning.

On MRI, piCCA manifests as periductal thickening and is T1 hypointense. It enhances most prominently in the delayed phase with variable degrees of arterial and venous phase enhancement (11). Periductal enhancement strongly correlates with periductal and perineural spread (0.93) and improves not only diagnostic accuracy and but also assessment of resectability when coupled with MRCP (53). Lesions may be T2 hypo- or hyperintense, depending on the amount of associated sclerosis or fibrosis (11). In its early stages, piCCA may be mistaken for a benign stricture. However, bile duct wall thickening greater than 5 mm, irregular outer margins, and abrupt or asymmetric narrowing are morphologic features more likely to be seen with malignancy (30,43). Functional features such as diffusion hyperintensity and hypervascularity on arterial and portal venous phase imaging are also indicative of malignancy. In fact, the presence of restricted diffusion on DWI with a b value =800 s/mm^2 is highly specific for malignant stricturing, even more so than the hypervascularity on contrast-enhanced MRI (30).

Intraductal-Growth Subtype (iCCA) (Figure 4)

The intraductal-growth subtype of intrahepatic cholangiocarcinoma (iCCA) represents 8–18% of all types of cholangiocarcinomas. It is considered a low-grade malignancy and carries the best prognosis of all intrahepatic cholangiocarcinomas because of its confined intraductal location (8). Most of these tumors exhibit papillary growth characteristics and proliferate toward the lumen with preservation of the bile duct wall and absence of parenchymal extension (2,8). Preservation of the bile duct wall without extension into the surrounding liver parenchyma distinguish this morphologic subtype from the periductal-infiltrating and mass-forming subtypes (49).

US

On ultrasound, iCCA usually presents as a intraductal mass resulting in alteration of biliary ductal caliber, usually ductal ectasia. The mass is typically polypoid hyperechoic (8,18). The lesion is usually confined to the wall of the bile duct (23). The presence of abundant anechoic mucin may, however, obscure visualization of an intraductal mass (23).

CT

On CT, iCCA may present in four distinct ways: (1) diffuse ductal ectasia with or without a visible intraductal mass, (2) intraductal polypoid mass with associated focal duct ectasia, (3) intraductal cast-like lesion within a slight dilated duct, or (4) a stricture with proximal ductal dilatation. Frequently, there is segmental ductal dilatation out of proportion to tumor size due to the production of abundant mucin, which is slightly higher in attenuation than simple bile (37,54,55). Multifocal intraductal papillary masses, known as papillomatosis or cholangiocarcinomatosis, may be present due to superficial tumor spread (8,24). When tumors get larger than 1 cm, an obstructing hypoattenuating mass may be visible (38).

Because of its confined intraductal location, iCCA may be confused with an intraductal stone. Frequently, the two findings coexist (24). High attenuation of non-contrast CT and absence of enhancement after contrast administration are useful distinguishing characteristics of a stone rather than a mass (19,52).

MRI/MRCP

MRCP is superior to CT for detection of iCCA (8). On MRI, iCCA presents as a polypoid or sessile intraductal mass with proximal ductal dilatation secondary to tumor obstruction or abundant mucin production (8). They are usually T2 hyperintense and T1 hypointense (23). After contrast administration, a nodular, well-defined mass with intense delayed enhancement is often visible (49). The pattern of contrast enhancement is similar to the mass-forming subtype, with heterogeneous early enhancement that peaks on the delayed phase (8,49). As previously stated,

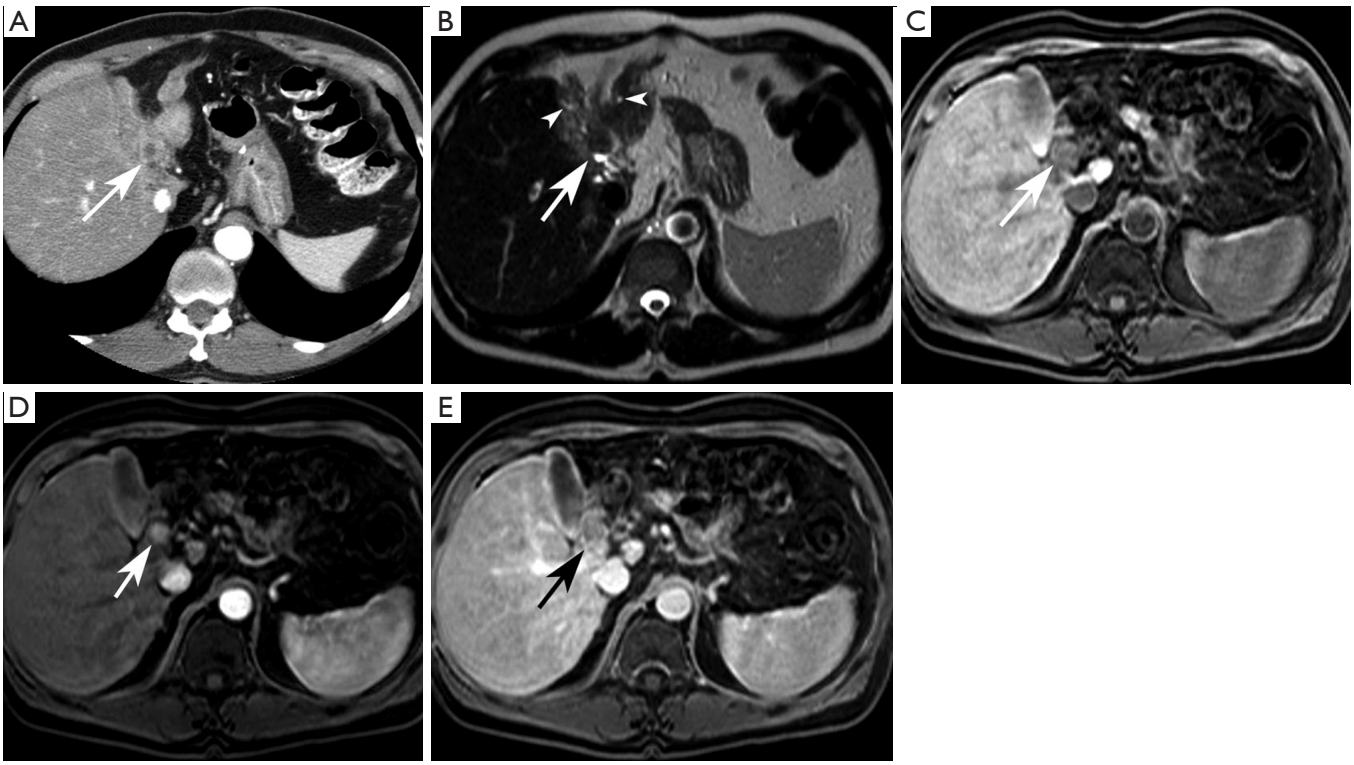

Figure 4 Intraductal-growth cholangiocarcinoma in a 67-year-old male. (A) Transverse post-iodinated contrast CT image in the portal venous phase shows a rim enhancing soft tissue mass (arrow) with marked atrophy of the left hepatic lobe; (B) T2-weighted image shows an intraductal mass (arrow) causing mild biliary ductal dilatation (arrowheads); (C) transverse fat saturated T1-weighted MR image without gadolinium chelate shows a hypointense mass (arrow). On fat saturated post-gadolinium chelate T1-weighted image (D), the mass is hypervascular (arrow) in the arterial phase, becoming slightly hypointense to liver parenchyma in the portal venous phase (E).

these masses may produce abundant mucin resulting in biliary obstruction and mass-like biliary ductal dilatation mimicking biliary cystadenocarcinoma (8,49).

Summary

In summary, three morphologic subtypes of intrahepatic cholangiocarcinoma exist, including mass-forming, periductal infiltrating, and intraductal subtypes. Each of these morphologic subtypes has a distinct imaging appearance on ultrasound (US), computed tomography (CT), and magnetic resonance imaging/magnetic resonance cholangiopancreatography (MRI/MRCP). Knowledge of the imaging appearances of each subtype facilitates diagnosis and timely management. Current of active research include the diagnostic and prognostic role of DW-MRI and the use of gadolinium-based contrast agents that combine properties of conventional extracellular and hepatocyte-specific agents.

Acknowledgements

None.

Footnote

Conflicts of Interest: The authors have no conflicts of interest to declare.

References

1. Kim NR, Lee JM, Kim SH, et al. Enhancement characteristics of cholangiocarcinomas on mutiphasic helical CT: emphasis on morphologic subtypes. Clin Imaging 2008;32:114-20.
2. Hennedige TP, Neo WT, Venkatesh SK. Imaging of malignancies of the biliary tract- an update. Cancer Imaging 2014;14:14.
3. Blechacz BR, Gores GJ. Cholangiocarcinoma. Clin Liver

Dis 2008;12:131-50, ix.
4. Poultsides GA, Zhu AX, Choti MA, et al. Intrahepatic cholangiocarcinoma. Surg Clin North Am 2010;90:817-37.
5. Dohan A, Faraoun SA, Barral M, et al. Extra-intestinal malignancies in inflammatory bowel diseases: an update with emphasis on MDCT and MR imaging features. Diagn Interv Imaging 2015;96:871-83.
6. Bader TR, Semelka RC, Reinhold C, Semelka RC, editors. Abdominal-pelvic MRI. New York: Wiley-Liss. Gallbladder and biliary system 2002:319-72.
7. Jiang L, Tan H, Panje CM, et al. Role of 18F-FDG PET/CT Imaging in Intrahepatic Cholangiocarcinoma. Clinical Nuclear Medicine 2016;41:1-7.
8. Jhaveri KS, Hosseini-Nik H. MRI of cholangiocarcinoma. J Magn Reson Imaging 2015;42:1165-79.
9. Liver Cancer Study Group of Japan (eds.) Classification of primary liver cancer, first English edition. Kanehara, Tokyo 2. 1997.
10. Han JK, Choi BI, Kim AY, et al. Cholangiocarcinoma: pictorial essay of CT and cholangiographic findings. Radiographics 2002;22:173-87.
11. Fowler KJ, Saad NE, Linehan D. Imaging approach to hepatocellular carcinoma, cholangiocarcinoma, and metastatic colorectal cancer. Surg Oncol Clin N Am 2015;24:19-40.
12. Liu GJ, Wang W, Lu M-D, et al. Contrast-enhanced ultrasound for the characterization of hepatocellular carcinoma and intrahepatic cholangiocarcinoma. Liver Cancer 2015;4:241-52.
13. Xu HX, Chen LD, Liu LN, et al. Contrast-enhanced ultrasound of intrahepatic cholangiocarcinoma: correlation with pathological examination. Br J Radiol 2012;85:1029-37.
14. Kleemann M, Hildebrand P, Birth M, et al. Laparoscopic ultrasound navigation in liver surgery: technical aspects and accuracy. Surg Endosc 2006;20:726-9.
15. Patel NA, Roh MS. Utility of intraoperative liver ultrasound. Surg Clin North Am 2004;84:513-24.
16. Xing G, Chen G, Peng X. The application of intraoperative ultrasound during partial hepatectomy for the accurate detection and removal of intrahepatic bile duct stones. Cell Biochem Biophys 2011;61:449-52.
17. Zacharoulis D, Asopa V, Navarra G, et al. Hepatectomy using intraoperative ultrasound-guided radiofrequency ablation. Int Surg 2003;88:80-2.
18. Chung YE, Kim MJ, Park YN, et al. Varying appearances of cholangiocarcinoma: radiologic-pathologic correlation. Radiographics 2009;29:683-700.
19. Lacomis JM, Baron RL, Oliver JH 3rd, et al. Cholangiocarcinoma: delayed CT contrast enhancement patterns. Radiology 1997;203:98-104.
20. Johnson PT, Fishman EK. Routine use of precontrast and delayed acquisitions in abdominal CT: time for change. Abdom Imaging 2013;38:215-23.
21. Zhang Y, Uchida M, Abe T, et al. Intrahepatic peripheral cholangiocarcinoma: comparison of dynamic CT and dynamic MRI. J Comput Assist Tomogr 1999;23:670-7.
22. Tada H, Morimoto M, Shima T, et al. Progressive jaundice due to lymphangiosis carcinomatosa of the liver: CT appearance. J Comput Assist Tomogr 1996;20:650-2.
23. Lim JH, Park CK. Pathology of cholangiocarcinoma. Abdom Imaging 2004;29:540-7.
24. Kawakatsu M, Vilgrain V, Zins M, et al. Radiologic features of papillary adenoma and papillomatosis of the biliary tract. Abdom Imaging 1997;22:87-90.
25. Fujita N, Asayama Y, Nishie A, et al. Mass-forming intrahepatic cholangiocarcinoma: Enhancement patterns in the arterial phase of dynamic hepatic CT - Correlation with clinicopathological findings. Eur Radiol 2017;27:498-506.
26. Bonekamp, S; Corona-Villalobos, CP; Halappa, VG; Kamel, IR. MR (Including MR Cholangiopancreatography). In: Herman, JM; Pawlik, TM; Thomas, Jr. CR; editors. Biliary Tract and Gallbladder Cancer. 2nd ed. Springer 2014;145-58. Available online: http://www.springer.com/us/book/9783642405570
27. Sheng RF, Zeng MS, Rao SX, et al. MRI of small intrahepatic mass- forming cholangiocarcinoma and atypical small hepatocellular carcinoma (3 cm) with cirrhosis and chronic viral hepatitis: a comparative study. Clinical Imaging 2014;38:265-72.
28. Fattach HE, Dohan A, Guerrache Y, et al. Intrahepatic and hilar mass-forming cholangiocarcinoma: Qualitative and quantitative evaluation with diffusion-weighted MR imaging. Eur J Radiol 2015;84:1444-51.
29. Park HJ, Kim YK, Park MJ, et al. Small intrahepatic mass-forming cholangiocarcinoma: target sign on diffusion-weighted imaging for differentiation from hepatocellular carcinoma. Abdom Imaging 2013;38:793-801.
30. Park HJ, Kim SH, Jang KM, et al. The role of diffusion-weighted MR imaging for differentiating benign from malignant bile duct strictures. Eur Radiol 2014;24:947-58.
31. Lee J, Kim SH, Kang TW, et al. Mass-forming Intrahepatic Cholangiocarcinoma: Diffusion-weighted Imaging as a Preoperative Prognostic Marker. Radiology 2016;281:119-28.

32. Ringe KI, Wacker F. Radiological diagnosis in cholangiocarcinoma: application of computed tomography, magnetic resonance imaging, and positron emission tomography. Best Practice & Research Clinical Gastroenterology 2015;29:253-65.
33. Petrowsky H, Wildbrett P, Husarik DB, et al. Impact of integrated positron emission tomography and computed tomography on staging and management of gallbladder cancer and cholangiocarcinoma. J Hepatol 2006;45:43-50.
34. Breitenstein S, Apestegui C, Clavien PA. Positron emission tomography (PET) for cholangiocarcinoma. HPB (Oxford) 2008;10:120-1.
35. Park MS, Lee SM. Preoperative 18F-FDG PET-CT Maximum Standardized Uptake Value Predicts Recurrence of Biliary Tract Cancer. Anticancer Research 2014;34:2551-4.
36. Vilgrain V, Van Beers BE, Flejou JF, et al. Intrahepatic cholangiocarcinoma: MRI and pathologic correlation in 14 patients. J Comput Assist Tomogr 1997;21:59-65.
37. Brant WE, Helms CA. Fundamentals of Diagnostic Radiology. Philadelphia: Lippincott-Williams 2012;886-7. Available online: https://www.amazon.com/Fundamentals-Diagnostic-Radiology-Set-Brant/dp/1608319121
38. Sainani NI, Catalano OA, Holalkere NS, et al. Cholangiocarcinoma: current and novel imaging techniques. Radiographics 2008;28:1263-87.
39. Valls C, Guma A, Puig I, et al. Intrahepatic peripheral cholangiocarcinoma: CT evaluation. Abdom. Imaging 2000;25:490-6.
40. Asayama Y, Yoshimitsu K, Irie H, et al. Delayed-phase dynamic CT enhancement as a prognostic factor for mass-forming intrahepatic cholangiocarcinoma. Radiology 2006;238:150-5.
41. Itai Y, Ohtomo K, Kokubo T, et al. CT of hepatic masses: significance of prolonged and delayed enhancement. AJR. Am. J. Roentgenol 1986;146:729-33.
42. Soyer P, Bluemke DA, Vissuzaine C, et al. CT of hepatic tumors: prevalence and specificity of retraction of the adjacent liver capsule. AJR Am J Roentgenol 1994;162:1119-22.
43. Soyer P, Pelage JP, Zidi SH, et al. Portal vein invasion by intrahepatic peripheral cholangiocarcinoma: a rare cause of portal hypertension. AJR Am J Roentgenol 1998;171:1413-4.
44. Worawattanakul S, Semelka RC, Noone TC. Cholangiocarcinoma: spectrum of appearances on MR images using current techniques. Magn Reson Imaging 1998;16:993-1003.
45. Park HS, Lee JM, Kim SH, et al. CT Differentiation of cholangiocarcinoma from periductal fibrosis in patients with hepatolithiasis. AJR Am J Roentgenol 2006;187:445-53.
46. Feng ST, Wu L, Huasong C, et al. Cholangiocarcinoma: spectrum of appearances on Gd-EOB-DTPA-enhanced MR imaging and the effect of biliary function on signal intensity. BMC Cancer 2015;15:38.
47. Kim SH, Lee CH, Kim BH, et al. Typical and atypical findings of intrahepatic cholangiocarcinoma using gadolinium ethoxybenzyl diethylenetriamine pentacetic acid-enhanced magnetic resonance imaging. J Comput Assist Tomogr 2012;36:704-9.
48. Laing FC. The gallbladder and bile ducts. In: Rumack CM, Wilson SR, Charboneau JW, eds. Diagnostic ultrasound. 2nd ed. St Louis, Mo: Mosby-Year Book. 1998;1;175-223.
49. Valls C, Ruiz S, Martinez L, et al. Radiological diagnosis and staging of hilar cholangiocarcinoma. World J Gastrointest Oncol 2013;5:115-26.
50. Manfredi R, Barbaro B, Masselli G, et al. Magnetic resonance imaging of cholangiocarcinoma. Semin. Liver Dis 2004;24:155-64.
51. Robledo R, Muro A, Prieto ML. Extrahepatic bile duct carcinoma: US characteristics and accuracy in demonstration of tumors. Radiology 1996;198:869-73.
52. Neitlich JD, Topazian M, Smith RC, et al. Detection of choledocholithiasis: comparison of unenhanced helical CT and endoscopic retrograde cholangiopancreatographay. Radiology 1997;203:753-7.
53. Ayuso JR, Pagés M, Darnell A. Imaging bile duct tumors: staging. Abdom Imaging 2013;38:1071-81.
54. Honda H, Onitsuka H, Yasumori K, et al. Intrahepatic peripheral cholangiocarcinoma: two-phased dynamic incremental CT and pathologic correlation. J Comput Assist Tomogr 1993;17:397-402.
55. Pavone P, Laghi A, Passariello R. MR cholangiopancreatography in malignant biliary obstruction. Semin Ultrasound CT MR 1999;20:317-23.

Cite this article as: Fábrega-Foster K, Ghasabeh MA, Pawlik TM, Kamel IR. Multimodality imaging of intrahepatic cholangiocarcinoma. HepatoBiliary Surg Nutr 2017;6(2):67-78. doi: 10.21037/hbsn.2016.12.10

